

## Photopolymerization of Organic Molecular Crystal Nanorods

Rabih O. Al-Kaysi,<sup>†,‡</sup> Robert J. Dillon,<sup>†</sup> J. Michael Kaiser,<sup>†</sup> Leonard J. Mueller,<sup>†</sup> Gonzalo Guirado,<sup>§</sup> and Christopher J. Bardeen<sup>\*,†</sup>*Department of Chemistry, University of California, Riverside, California 92521, and Department of Chemistry, University Autònoma of Barcelona, 08193-Bellaterra, Barcelona, Spain**Received July 30, 2007; Revised Manuscript Received September 19, 2007*

**ABSTRACT:** The dianthracene molecule 9-anthracenecarboxylic acid, methylene ester (9AC-ME) was synthesized and used to form molecular crystal nanorods using anodized aluminum oxide templates. A high-temperature solvent annealing process generated a crystal polymorph where neighboring monomers had overlapping anthracene moieties. Subsequent exposure to ultraviolet light caused the monomers to undergo a [4 + 4] photocycloaddition reaction, forming highly crystalline polymer nanorods of poly(9AC-ME). The polymer nanorods are flexible, resistant to breakage, and insoluble in organic solvents and strong acid/base solutions. Their molecular structure is characterized by powder X-ray diffraction, solid-state NMR, and UV–vis spectroscopy. Different diameter crystalline polymer nanorods could be fabricated using alumina templates of variable pore diameter.

## Introduction

The ability to make nanostructures composed of organic molecules may lead to both novel materials and new types of physical phenomena. Polymeric materials are of particular interest due to their widespread application and unique physical properties. The most commonly made polymer nanostructures are one-dimensional fibers or wires, which have potential applications in biomedical engineering and materials science.<sup>1,2</sup> A widely used and versatile way to make polymer nanofibers is the electrospinning method, which is used to produce nanofibers with lengths on the order of hundreds of micrometers and diameters down to  $\sim 1$  nm.<sup>3</sup> Polymer electrospinning requires that the polymer be processed from liquid solution, which makes it difficult to use with insoluble or cross-linked polymers. An alternate method for making polymer nanofibers is via templated growth.<sup>4</sup> Several groups have used electrochemical polymerization of monomers inside anodic aluminum oxide (AAO) porous templates to make nanowires out of conjugated polymers.<sup>5–7</sup> Attempts to directly fill the channels of AAO templates with polymers from solution or a melt usually result in hollow tubes rather than solid rods,<sup>8–10</sup> although confinement-induced effects in block copolymers can be used to produce a wide variety of structures.<sup>11,12</sup> Both electrospinning and templated electrochemical polymerization tend to result in amorphous or highly polycrystalline solids, although there exist methods to at least partially align the chains within the fiber.<sup>13</sup> Our group has recently developed a way to grow organic molecular crystal nanorods by slow solvent annealing of small molecule-filled AAO templates.<sup>14</sup> We have demonstrated that photodimerization of the molecules in such a rod can lead to a crystal-to-crystal transition to the photodimer crystal, with concomitant expansion and deformation of the intact rod to accommodate the new phase.<sup>15,16</sup> This photodimerization reaction proceeds in the nanorod without the disruption and fragmentation commonly seen in larger crystals. Other results

on diolefin photopolymerization and [2 + 2] photodimerization have also provided evidence for the ability of nanostructures to undergo solid-state photochemistry without fragmentation.<sup>17,18</sup> We decided to investigate whether a crystalline nanorod can undergo a crystal-to-crystal photopolymerization,<sup>19</sup> which would open up the possibility of making crystalline polymer structures with uniform shapes and sizes.

To demonstrate crystal-to-crystal photopolymerization in a shaped nanostructure, we synthesized the molecule 9-anthracenecarboxylic acid, methylene ester (9AC-ME), whose structure is shown in Figure 1. By choosing the appropriate conditions, we were able to grow crystalline nanorods of this molecule which can undergo photopolymerization between adjacent monomers to form the polymer poly(9AC-ME). We characterize the monomer and polymer rods and demonstrate the ability to tune their diameter by using different AAO templates. Attempts to accomplish this photochemical transformation using other types of media, like liquid solution or macroscopic single crystals, resulted in either poorer results or no reaction at all. Thus the nanorods not only provide a way to make a polymer structure of well-defined size and shape, they also provide highly ordered, solvent-free conditions which are necessary for the reaction to proceed in a concerted fashion with high yield. This work extends earlier results showing the utility of nanoscale crystals for solid-state chemical transformations.

## Experimental Section

**Synthesis of 9AC-ME Monomer.** In an oven dried 50 mL round-bottom flask, 9-anthracene carboxylic acid (9-AC, 1.0 g, 4.5 mM) was added to 6 mL of dry *N,N*-dimethylformamide (DMF). The 9-AC was dissolved, and then anhydrous  $K_2CO_3$  (2.5 g, 18 mM) was added along with a couple of KI crystals as a catalyst. The mixture was gently agitated at room temperature for several minutes before adding dibromomethane (10 g, 52 mM, 11.5 equiv). The mixture was stirred at 50 °C under an argon atmosphere for 24 h. Distilled water (35 mL) was added to dissolve the excess  $K_2CO_3$  and KBr salts, after which a heavy dark oily residue separated out and was collected. The aqueous phase was extracted with 15 mL of  $CH_2Cl_2$ . The organic extract was combined with the oily residue and dried using anhydrous  $MgSO_4$ . The organic solvent and excess dibromomethane were removed under reduced pressure. We obtained 0.9 g of crude yellow brown solid. The crude product was recrystallized twice from acetonitrile (50 mL), to give

\* To whom correspondence should be addressed. E-mail: christopher.bardeen@ucr.edu.

<sup>†</sup> University of California.

<sup>‡</sup> Current address: Assistant Professor of Chemistry, College of Medicine, King Saud bin Abdulaziz University for Health Science, National Guard Health Affairs, Riyadh, Kingdom of Saudi Arabia.

<sup>§</sup> University Autònoma of Barcelona.

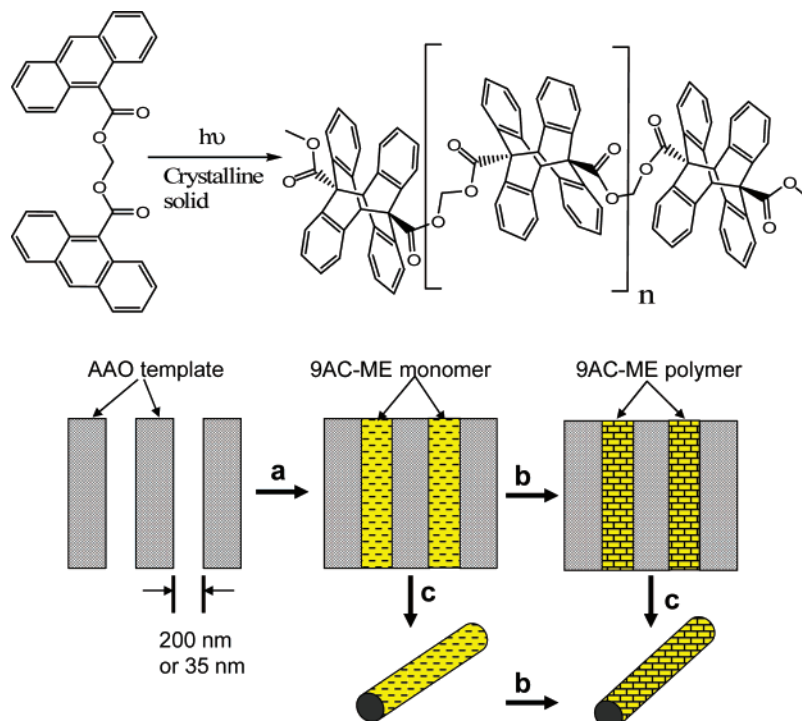


**Figure 1.** Top, photopolymerization reaction scheme of 9AC-ME in the crystalline solid state. Bottom, scheme for the preparation of 9AC-ME monomer and polymer nanorods: (a) growth of 9AC-ME nanorods in AAO template using solvent annealing with THF at 68 °C; (b) irradiation using UV light ( $\lambda > 365$  nm); (c) dissolve the alumina template using 50% aqueous  $H_3PO_4$ .

0.8 g of pure yellow crystals (80% yield). Melting point (uncorrected) = 193–194 °C.  $^1H$  NMR (400 MHz,  $CDCl_3$ ):  $\delta_{ppm}$  = 6.73 (s, 2H), 7.48 (m, 8H), 8.04 (d, 4H), 8.15 (d, 4H), 8.59 (s, 2H).  $^{13}C$  NMR ( $CDCl_3$ ):  $\delta_{ppm}$  = 81.32 (methylene carbon), 125.09, 125.78, 126.13, 127.64, 128.88, 128.95, 130.49, 131.11, 168.46 (C=O). High-resolution mass spectrum:  $M^+$  = 456.1367.

**Synthesis of the 9AC-ME Monomer Nanorods and Polymer Nanorods.**<sup>14</sup> A saturated solution of the 9AC-ME in tetrahydrofuran (THF 10 mg/0.15 mL) was deposited over commercially available alumina Anodisc filters (Whatman Ltd., Anodisc 13 with a 200 nm quoted diameter and 60  $\mu m$  thick membrane) or custom-made anodized alumina templates purchased from Synkera (35 nm pore diameter, 50  $\mu m$  thick). The loaded alumina template was placed on top of a special Teflon holder and then placed inside a 150 mL capacity jar padded with cotton and soaked with 7 mL of THF. The jar was tightly sealed by capping it with aluminum foil and sealing the sides with Teflon tape. The jar was then placed inside an oven set at 68 °C for a period of 15 h or until all the solvent evaporated. Finally, the Anodisc was polished with 2000 grit sandpaper to remove excess monomer. The polishing leaves a thin crust of monomer on the template surface as seen previously for 9-tertbutyl anthracene ester.<sup>15</sup> The rods, which are inside the template, are not affected by the polishing. Photopolymerization of the 9AC-ME could be accomplished using nanorods either inside the template or suspended in aqueous solution. In the first case, a loaded template was placed under a 15 W mercury lamp for at least 8 h. The same photopolymerization could be achieved by exposing the loaded template to sunlight for 5–8 h under glass. The template was then repolished using 2000 grit sandpaper and dissolved using 50% aqueous  $H_3PO_4$  solution. The polymer nanorods could be isolated from the acidic solution by centrifuging and washing repeatedly with water. Alternatively, the monomer 9AC-ME rods could be liberated from the template by dissolving it with 50% aqueous  $H_3PO_4$  solution and then photopolymerized under the same illumination conditions. The isolated rods react more rapidly since the template is no longer present to scatter the UV photons. In either case, the resulting polymer nanorods could be resuspended in a variety of organic solvents without dissolving. Washing the polymer nanorods with dichloromethane did not yield

a measurable amount of unreacted 9AC-ME monomer in the organic phase.

**Synthesis of Crystalline Bulk 9AC-ME Polymer.** Large crystals of 9AC-ME could be obtained by THF solvent annealing at 68 °C in the absence of a template. When exposed to UV light for several hours, the crystals change color and turn to powder. The polymer powder was washed with dichloromethane to remove the unreacted monomer, with a final yield for the insoluble polymer of 76%. When 9AC-ME crystals were grown from slow evaporation of THF solution at room temperature (20 °C), they were found to be photostable. Washing these crystals after exposure to UV light resulted in an estimated yield for polymer formation of less than 5%, as estimated from the mass of the undissolved solid. Poly(9AC-ME) can also be formed by irradiation of a 9AC-ME solution. Monomeric 9AC-ME (85 mg) was dissolved in 2 mL of dichloromethane and 1 mL of benzene (concentration of monomer = 0.062 M), purged with argon, then tightly sealed in a 4 mL vial. The solution was exposed to sunlight (only wavelengths greater than 300 nm were able to penetrate the glass) for one week. During this period, a gel formed which was collected and washed with dichloromethane. The amount of insoluble polymer left after washing and drying was found to be 73 mg (86% yield).

**Characterization of Products.** For powder X-ray diffraction (XRD) measurements, roughly 30 mg samples of the bulk poly(9AC-ME) were pulverized using an agate mortar and pestle and spread evenly on a polycarbonate sample holder. For polymer nanorod samples, methanol suspensions were placed on the holder, and after evaporation of the solvent, more solution was added until a sufficient amount for obtaining reasonable XRD signals was accumulated. The samples were scanned over a wide range, typically between 5 and 70° at a scan rate of 0.1°/s, using a Bruker D8 Advance diffractometer with Cu K $\alpha$  radiation (40 kV, 40 mA). For scanning electron microscopy (SEM), a drop of the poly(9AC-ME) nanorod–water suspension was placed on a copper tape and fixed on an SEM stub. The water was slowly evaporated, leaving behind a dispersed network of polymer nanorods. The SEM stub was placed in a sputter coater (Cressington 108 Auto) and coated with Pt/Au for a cycle of 40 s. The SEM stub was then placed



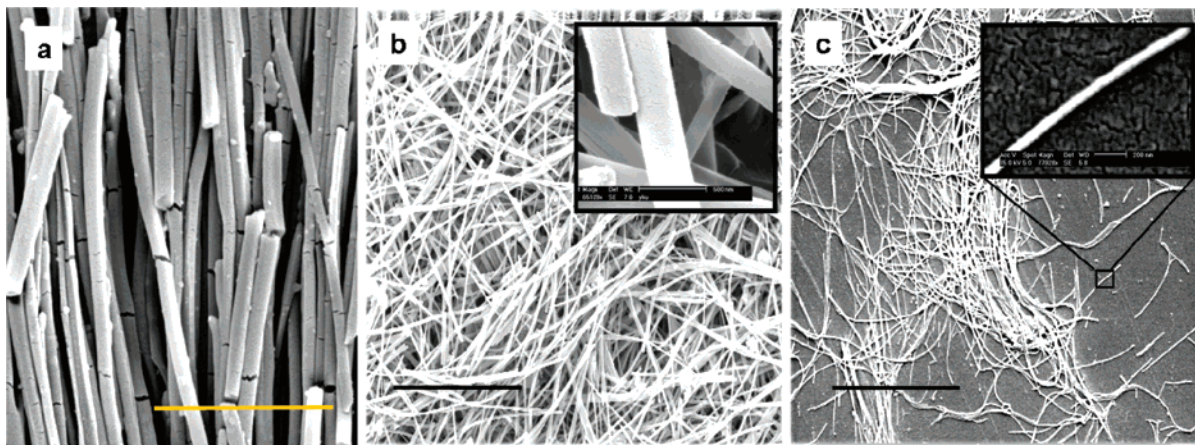


**Figure 2.** SEM images of 9AC-ME monomer and poly(9AC-ME) nanorods: (a) 9AC-ME monomer nanorods (scale = 2.5  $\mu\text{m}$ ). The monomer nanorods are brittle hence the breakage due to electron beam damage. (b) Polymer nanorods made using 200 nm pore diameter templates (scale = 8  $\mu\text{m}$ ). Inset: individual nanorods (scale = 500 nm). (c) Nanorods made using 35 nm pore diameter templates (scale = 8  $\mu\text{m}$ ). Inset: individual nanorod (scale = 200 nm).

inside a scanning electron microscope (the XL30 FEG), and the data were collected using a 15 kV electron beam.

Absorption spectra of the nanorod solids were measured for thin solid films on a fused silica substrate using a Cary 500 spectrophotometer. The fluorescence was measured using an aqueous suspension of nanorods with a Jobin Yvon Spex Fluorolog Tau-3 fluorescence spectrophotometer. Since each nanorod sample yielded less than 1 mg of nanorods, we had to use bulk crystals for the NMR measurements.  $^{13}\text{C}$  solid-state NMR spectra were acquired at 9.4 T on a Bruker DSX spectrometer ( $^1\text{H}$  frequency 400.1 MHz) equipped with a double resonance 4 mm magic-angle-spinning probe spinning at 10 kHz. Cross-polarization<sup>20</sup> from  $^1\text{H}$  to  $^{13}\text{C}$  was incorporated using a 4 ms 40 kHz spin lock on  $^{13}\text{C}$  and a linearly ramped (50%–100%) matching field on  $^1\text{H}$ . In the experiment, 1024 complex time points with a dwell of 20  $\mu\text{s}$  (spectral width 50 kHz, total acquisition time 20.48 ms) were acquired with a recycle delay of 3 s. For the polymer, approximately 40 mg of photopolymerized sample were center packed in the rotor and 1024 scans co-added for a total experiment time of 0.9 h. For the monomer, approximately 15 mg of sample were center packed in the rotor and 4096 scans co-added for a total experiment time of 3.6 h.

## Results and Discussion

The basic synthetic scheme is outlined in Figure 1. The monomer nanorods are prepared by placing a few drops of saturated 9AC-ME solution on the AAO template. The template is then placed in a closed chamber with some THF and heated just above the solvent boiling point. As the solvent slowly escapes from the container, the crystalline rods grow within the template channels. The photopolymerization of dianthracenes in solution has been observed,<sup>21,22</sup> and we found that the same reaction can also occur in the solid state using illumination at wavelengths below 400 nm. Illumination can be done either before or after liberating the rods by dissolving the  $\text{Al}_2\text{O}_3$  template with concentrated phosphoric acid. When irradiated, the liberated monomer rods are observed to lengthen and change color. The green excimer fluorescence, originating from the  $\pi$ -stacked anthracene chromophores, is replaced by a faint blue fluorescence. This residual fluorescence likely originates from a small concentration of unreacted monomers trapped in the polymer crystal matrix.<sup>23</sup> For individual rods observed under a fluorescence microscope, some flexing and bending of the rod often accompanies the color change as the rod is exposed to light. The entire transformation is complete within 1 s, resulting in a straight rod, as before, but now lengthened by 3–5%. Presumably, the increase in length is due to expansion of the

product unit cell along the dimension aligned with the rod axis, as in the case of 9-*tert*butyl anthracene ester.<sup>15</sup>

The SEM image in Figure 2a confirms that the 9AC-ME monomer forms solid rods within the AAO channels, as we have seen before for a variety of other molecules.<sup>14</sup> The solid cross section of the rods, observed both at the ends and where breaks occur, shows no sign of shell- or tubelike growth. The photopolymerized rods are also solid and furthermore can be formed using AAO templates of varying diameters. Two different sizes are shown in Figure 2b,c, made using 35 and 200 nm pore diameter templates. With the use of commercially available templates, diameters down to 13 nm should be achievable. Note that the diameters of the nanorods in Figure 2 (~230 and ~50 nm) are slightly greater than the nominal template pore diameters due to the additional thickness of the sputter coating. The nanorods made using this method have the additional advantage that they can be produced while aligned in the template, as opposed to the random tangle produced by electrospinning. The polymer rods produced photochemically are transparent in the visible and near-ultraviolet and are completely insoluble in hot or cold organic solvents ( $\text{CH}_2\text{Cl}_2$ ,  $\text{CHCl}_3$ , THF, *N,N*-dimethylformamide) as well as aqueous solutions where the pH ranges between 2 and 12. The insolubility of the sample makes determining the polymer molecular weight using gel permeation chromatography impossible. They are also highly resistant to breakage. Under sonication conditions that typically snap 60  $\mu\text{m}$  long monomer rods into shorter segments, the polymer rods remain intact, as judged by the absence of lengths shorter than 60  $\mu\text{m}$  when viewed under an optical microscope or SEM.

We have found that 9AC-ME can crystallize into two different polymorphs, which are shown in parts a and b of Figure 3. Under the high-temperature solvent annealing conditions used here, the crystal polymorph that grows is a  $\pi$ -stacked type where the stacked anthracenes alternate from molecule to molecule. This crystal structure is shown in Figure 3a and is of a type where the anthracenes of neighboring molecules have the correct spacing and alignment to undergo a [4 + 4] photocycloaddition reaction.<sup>24</sup> Only this type of crystal polymorph of 9AC-ME is able to support the polymerization reaction. It is formed under high-temperature crystallization conditions, as used in the rod solvent annealing process. The more stable crystal polymorph formed at room temperature, shown in Figure 3b, does not have the anthracene groups correctly oriented to

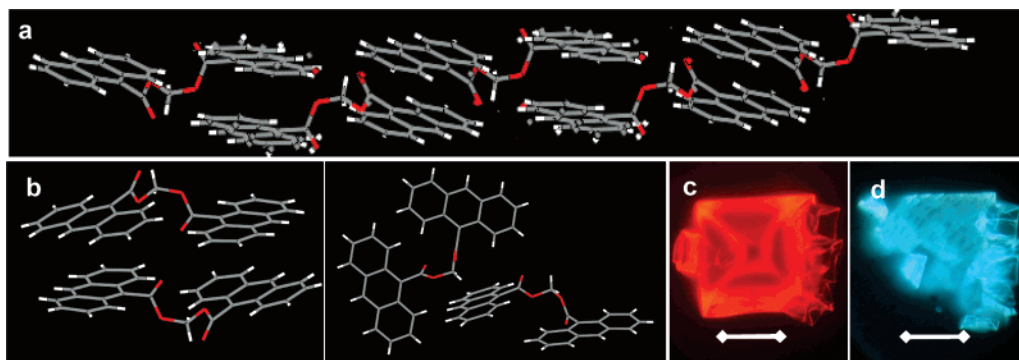


**Figure 3.** (a) Crystal structure of 9AC-ME monomer crystals solvent annealed from THF at 68 °C. The anthracene units of adjacent molecules stack in a parallel conformation, with the dianthracenes forming an alternating chain. (b) Two different crystal structure renderings of 9AC-ME monomer crystals grown from THF at room temperature. The anthracene units are not parallel and there is no alternation in the dianthracene stacks. (c) A single crystal of 9AC-ME monomer grown from THF at 68 °C before illumination with 365 nm light. The microscope color filter only transmits red light, so the crystal appears red. (d) After a brief illumination with 365 nm light, poly(9AC-ME) forms and the crystal shatters and turns fluorescent blue due to residual unreacted anthracene units. Scale bar = 45  $\mu\text{m}$ .

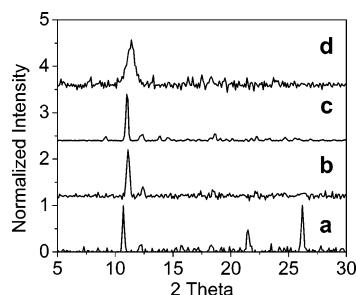


**Figure 4.** Normalized powder XRD of (a) 9AC-ME monomer nanorods, (b) poly(9AC-ME) polymer nanorods, (c) poly(9AC-ME) after bulk solid-state photopolymerization, and (d) poly(9AC-ME) after photopolymerization in solution.

support the  $[4 + 4]$  photodimerization, and this type of crystal is almost completely inert under the same irradiation conditions. An additional point is that this photoreaction must be done in the nanometer scale structure in order to preserve the intact shape of the precursor monomer crystal. Under identical irradiation conditions, a macroscopic crystal of 9AC-ME simply shatters, as shown in Figure 3c,d. This is consistent with previous observations by our group and others that a high surface-to-volume ratio helps alleviate the strain buildup that often occurs when a crystalline solid undergoes a photochemical reaction.<sup>25–27</sup>

The crystal-to-crystal nature of the photopolymerization is confirmed by powder XRD measurements. The powder XRD patterns of the monomer rods before irradiation and the polymer rods after irradiation are shown in Figure 4a,b. Both exhibit narrow diffraction lines and low amorphous background scattering, indicative of highly crystalline materials. For comparison, the powder XRD pattern of a polymerized macroscopic 9AC-ME crystal is shown in Figure 4c. Shown in Figure 4d is the XRD pattern of a solid obtained from solution photopolymerization of 9AC-ME in dichloroethane–benzene. Some aspects of the XRD patterns in Figure 4 should be highlighted. First, the patterns for the nanorod and bulk polymer crystals (Figure 4b,c) are the same to within the signal-to-noise. This confirms that the nanorod polymer solid is identical to that formed in the reaction in a macroscopic crystal. Second, the width of the diffraction peaks is limited by the instrument resolution in all cases except for Figure 4d. The broader peaks seen in the solution-grown polymer solid indicate greater disorder and smaller crystalline domains, on the order of 15 nm as estimated using the Scherrer equation.<sup>28</sup> Thus the solid-state reaction conditions in the monomer nanorod lead to significantly greater

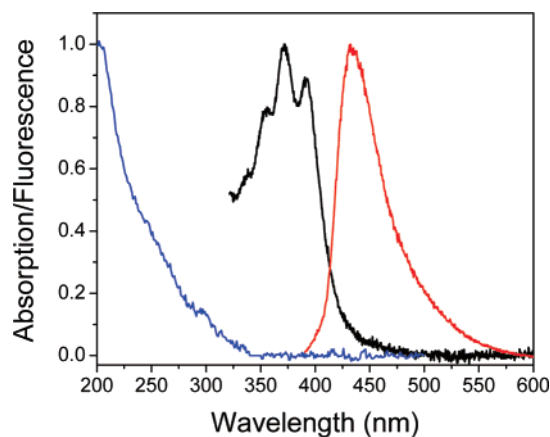


**Figure 5.** Normalized absorption (black) and fluorescence (red) of 9AC-ME monomer crystal nanorods and absorption of the photopolymer solid (blue).

crystallinity in the polymer rod, as opposed to what could be obtained from photopolymerization in solution. Whether the walls of the AAO channels exert any influence on the growth of the crystalline rods remains an open question. Since the radius of the 9AC-ME monomer is at least a factor of 50 less than the smallest channel diameter channel used, it is unlikely that the walls exert a large influence on the growth of the monomer nanorods, which also determines the alignment of the polymer nanorods. However, it is possible that there will be differences when very small diameter channels are used.

The powder XRD data can provide information about crystallinity, but the insolubility of the photopolymer makes it difficult to apply standard techniques to confirm the hypothesized molecular structure shown in Figure 1. We were unable to prepare a large single-crystal suitable for X-ray structure determination, and attempts to use solution NMR and mass spectrometry techniques were also unsuccessful. We turned to UV–vis spectroscopy and solid-state NMR to analyze the properties of the 9AC-ME solid before and after UV irradiation. Figure 5 shows the absorption and fluorescence spectra of the monomer nanorods. The well-resolved vibronic absorption spectrum starting at 400 nm is typical of the anthracene chromophore, while the lower energy, featureless emission spectrum is typical of anthracene excimer emission, as expected from the sandwich structure of the crystal shown in Figure 3a. After irradiation, the anthracene absorption completely disappears, replaced by a gradually rising absorption with very slight shoulders at around 300 and 250 nm, where the absorption of



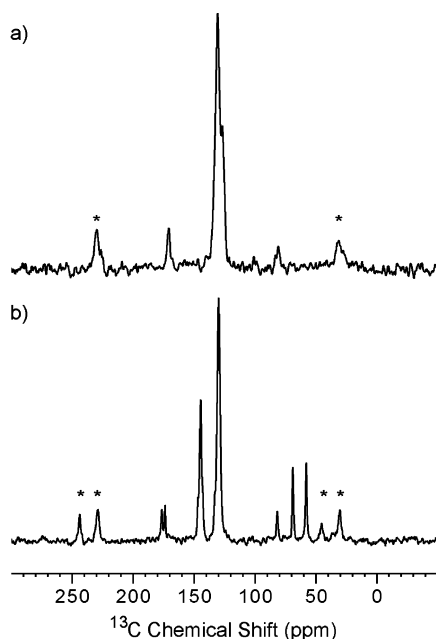


**Figure 6.** (a) Solid-state  $^{13}\text{C}$  NMR spectrum of the high-temperature polymorph monomer crystal of 9AC-ME. The three main features consist of a set of aromatic carbons centered at 130.5 ppm, CO at 170.5 ppm, and  $\text{CH}_2$  at 80.6 ppm. The spinning sidebands are marked with asterisks. (b) Solid state  $^{13}\text{C}$  NMR spectrum of the photopolymer. There are new bridge head aliphatic (57.7 ppm) and quaternary (68.7 ppm) carbons in addition to the  $\text{CH}_2$  at 80 ppm, a new type of aromatic carbon at 144.4 ppm, and the CO signal now shows two inequivalent carbons at 176.2 and 173.6 ppm.

the carbonyl and the benzene rings are expected. The absorption spectrum of the photopolymer probably also includes a contribution from scattering by the larger polymer particles. We could not detect fluorescence from the photopolymer sample. The UV-vis spectra confirm the loss of the anthracene in the photopolymerization. More detailed chemical information is obtained from the solid-state NMR spectra of the monomer before and after irradiation, which is shown in Figure 6. The monomer spectrum contains three main features: a set of aromatic peaks centered at 130.5 ppm which overlap with each other due to their similar electronic environments, a CO carbon peak at 170.5 ppm, and a  $\text{CH}_2$  linker peak at 80.6 ppm. The different types of carbon peaks can be identified by their standard chemical shifts.<sup>29</sup> After irradiation, several new peaks appear. First, the loss of the central aromatic ring in the anthracene gives rise to two types of inequivalent aromatic carbons in the remaining outer rings: four are next to the aliphatic carbons in the center and are shifted to 114.4 ppm, while eight of these carbons retain their original aromatic environments. Second, there appear two new aliphatic carbon peaks at 57.7 and 68.7 ppm. These two new peaks correspond to the inequivalent carbons created by the cyclization reaction in Figure 1. Finally, the photopolymerization appears to make the two CO carbons inequivalent, since the original single CO peak at 170.5 ppm now shifts and splits into two peaks at 173.6 and 176.2 ppm. All of these changes are consistent with the reaction mechanism shown in Figure 1, which is the only plausible mechanism given the crystal structure in Figure 3a. This data confirms the chemical structure of the polymer repeat unit, although determination of the overall chain structure and crystal packing remains a challenge.

## Conclusion

We have shown how a template-based solvent annealing method can be used to form crystalline nanorods of a dian-

thracene polymer precursor. Irradiation at wavelengths below 400 nm leads to a crystal-to-crystal photopolymerization, resulting in highly crystalline polymer nanorods with variable diameters, good mechanical properties, and high solvent resistance. This method provides a way to produce aligned samples of such rods, which may have applications in materials science or biomedical engineering. This work also illustrates how the use of nanoscale molecular crystals permits chemical transformations that are often impractical for macroscopic samples, and it is likely that other types of solid-state chemical reactions will also benefit from the use of these types of nanostructures.

**Acknowledgment.** C.J.B. acknowledges the support of the National Science Foundation, Grant CHE-0517095 and the University of California Energy Institute. L.J.M. acknowledges the support of the National Science Foundation, Grant CHE-0349345, and the National Institutes of Health, Grant S10RR023677. G.G. gratefully acknowledges the financial support of the Ministry of Technology and Science of Spain through Projects BQU 2003-05457 and CTQ2006-01040.

**Supporting Information Available:** Proton and carbon NMR of 9AC-ME monomer, different renderings of the photoreactive 9AC-ME crystal structure, SEM images of poly(9AC-ME) nanorods 200 and 35 nm, tables of X-ray diffraction data (cif files) of the different 9AC-ME polymorphs. This material is available free of charge via the Internet at <http://pubs.acs.org>.

## References and Notes

- Venugopal, J.; Ramakrishna, S. *Appl. Biochem. Biotechnol.* **2005**, *125*, 147–157.
- Subbiah, T.; Bhat, G. S.; Tock, R. W.; Parameswaran, S.; Ramkumar, S. S. *J. Appl. Polym. Sci.* **2005**, *96*, 557–569.
- Huang, C.; Chen, S.; Lai, C.; Reneker, D. H.; Qiu, H.; Ye, Y.; Hou, H. *Nanotechnology* **2006**, *17*, 1558–1563.
- Martin, C. R. *Science* **1994**, *266*, 1961–1966.
- Liang, W.; Martin, C. R. *J. Am. Chem. Soc.* **1990**, *112*, 9666–9668.
- Qu, L.; Shi, G. *Chem. Commun.* **2004**, 2800–2801.
- Berdichevsky, Y.; Lo, Y.-H. *Adv. Mater.* **2006**, *18*, 122–125.
- Cepak, V. M.; Martin, C. R. *Chem. Mater.* **1999**, *11*, 1363–1367.
- Steinhart, M.; Wendorff, J. H.; Wehrspohn, R. B. *ChemPhysChem* **2003**, *4*, 1171–1176.
- Zheng, R. K.; Yang, Y.; Wang, J.; Chan, H. L. W.; Choy, C. L.; Jin, C. G.; Li, X. G. *Chem. Commun.* **2005**, 1447–1449.
- Xiang, H.; Shin, K.; Kim, T.; Moon, S. I.; McCarthy, T. J.; Russell, T. P. *Macromolecules* **2004**, *37*, 5660–5664.
- Shin, K.; Xiang, H.; Moon, S. I.; Kim, T.; McCarthy, T. J.; Russell, T. P. *Science* **2004**, *306*, 76.
- Kakade, M. V.; Givens, S.; Gardner, K.; Lee, K. H.; Chase, D. B.; Rabolt, J. F. *J. Am. Chem. Soc.* **2007**, *129*, 2777–2782.
- Al-Kaysi, R. O.; Bardeen, C. J. *Chem. Commun.* **2006**, 1224–1226.
- Al-Kaysi, R. O.; Muller, A. M.; Bardeen, C. J. *J. Am. Chem. Soc.* **2006**, *128*, 15938–15939.
- Al-Kaysi, R. O.; Bardeen, C. J. *Adv. Mater.* **2007**, *19*, 1276–1280.
- Takahashi, S.; Miura, H.; Kasai, H.; Okada, S.; Oikawa, H.; Nakanishi, H. *J. Am. Chem. Soc.* **2002**, *124*, 10944–10945.
- Bucar, D.-K.; MacGillivray, L. R. *J. Am. Chem. Soc.* **2007**, *129*, 32–33.
- Hoyle, C. E.; Torkelson, J. M. *Photophysics of Polymers*; Hoyle, C. E., Torkelson, J. M., Eds.; Oxford University Press: New York, 1987.
- Sanders, J. K. M.; Hunter, B. K. *Modern NMR Spectroscopy*; Oxford University Press: Oxford, U.K., 1993.
- Tazuke, S.; Tanabe, T. *Macromolecules* **1979**, *12*, 848–853.
- Tazuke, S.; Tanabe, T. *Macromolecules* **1979**, *12*, 853–862.
- MacFarlane, R. M.; Philpott, M. R. *Chem. Phys. Lett.* **1976**, *41*, 33–36.
- Ramamurthy, V.; Venkatesan, K. *Chem. Rev.* **1987**, *87*, 433–481.
- Kaupp, G. *Angew. Chem., Int. Ed.* **1992**, *31*, 595–598.
- Keating, A. E.; Garcia-Garibay, M. A. *Photochemical Solid-to-Solid Reactions*, 1st ed.; Keating, A. E., Garcia-Garibay, M. A., Eds.; Dekker: New York, 1998; Vol. 2, pp 195–248.
- Turowska-Tyrk, I. *J. Phys. Org. Chem.* **2004**, *17*, 837–847.
- Guinier, A. *X-ray Diffraction*; W. H. Freeman & Co.: New York, 1963.
- Loudon, G. M. *Modern Organic Chemistry*; Addison-Wesley: Reading, MA, 1984.